scientific reports

Check for updates

OPEN

Alternative production of pro-death BaxΔ2 protein via ribosomal frameshift in Alzheimer's disease

Qi Yao[1], Adriana Mañas[2,3], Evan Beatty[1], Anne Caroline Mascarenhas dos Santos[1], Yi Zhou[1], Oscar Juárez[1], Hui Chen[4] & Jialing Xiang[1]✉

Pro-death Bax family member, BaxΔ2, forms protein aggregates in Alzheimer's disease neurons and causes stress granule-mediated neuronal death. Production of BaxΔ2 originated from two events: alternative splicing of Bax exon 2 and a microsatellite mutation (a deletion from poly guanines, G8 to G7). Each event alone leads to a reading frameshift and premature termination. While Bax exon 2 alternative splicing is common in Alzheimer's brains, the G7 mutation is not, which is inconsistent with the high BaxΔ2 protein levels detected in clinical samples. Here, we report an alternative mechanism to produce BaxΔ2 protein in the absence of the G7 mutation. Using dual-tag systems, we showed that a ribosomal frameshift (RFS) can compensate the lack of G7 mutation in translating BaxΔ2 protein. Intriguingly, the microsatellite poly G repeat is neither essential nor the site for the RFS. However, disruption of the poly G sequence impaired the RFS, potentially due to alteration of the local RNA structure. Using immunoprecipitation-mass spectrometry, we pinpointed the RFS site at 15 base pairs upstream of the microsatellite. These results uncover an alternative mechanism for generating functional BaxΔ2-subfamily isoforms, highlighting the production plasticity of Bax family isoforms and unveiling potential new therapeutic targets for Alzheimer's disease.

Keywords Bax, BaxΔ2, Cell death, Ribosomal frameshift, Alzheimer's disease, Microsatellite

The proapoptotic protein Baxα causes mitochondria-mediated cell death by forming an oligomer-pore ring on the mitochondrial outer membrane[1–4]. BaxΔ2, an alternatively-spliced Bax isoform, cannot target mitochondria, due to the lack of the targeting helix coded by exon 2[5,6]. Instead, it forms cytosolic protein aggregates that recruit and activate caspase 8, triggering mitochondria-independent apoptosis[7–9]. BaxΔ2 protein levels in normal human organs are low, with 1 ~ 5% of positive cells, which appears scattered in the connective tissues[10–12]. BaxΔ2 protein is unstable in cancer cells due to their elevated proteasomal degradation[13] and it is rarely detected in highly malignant tumors[11]. On the other hand, BaxΔ2 aggregates are readily detected in the brain of Alzheimer's disease (AD) patients, especially in AD-susceptible affected regions, with up to 30% of neurons being BaxΔ2-positive in AD patient's frontal lobes[14]. We also showed that the presence of BaxΔ2 aggregates in neurons can trigger the formation of stress granules (SGs), a large protein-RNA complex implicated in many neurodegenerative diseases[15,16]. BaxΔ2 interacts with SGs via its C-terminal end, the same region involved in its interaction with caspase 8 in cancer cells[9,14]. As a result, the BaxΔ2-mediated neuronal cell death is dependent on SGs but not on caspase 8[14].

Alternative splicing is highly associated with AD progression[17–19]. For example, RBFox is involved in regulation of the alternative splicing of *APP* exon 7 leading to the production of APP695, which increases beta-amyloid release[18,20]. Alternative splicing of *MAPT* exon 10 can cause imbalanced tau protein production, promoting tau protein aggregation[21,22]. Our previous studies also found that 85% of AD patients presented exon 2 alternative splicing, which is required to produce BaxΔ2[14]. Alternative splicing events are common within the Bax family, giving rise to many Bax isoforms[23–26]. However, alternative splicing of exon 2 alone leads to a reading frameshift and premature termination[5,6]. Intriguingly, such premature termination can be avoided by a mononucleotide deletion, which offsets the out-of-frame shift at the beginning of exon 3, restoring the remaining sequence equal to Baxα, including all critical domains for dimerization, oligomerization, and pro-death function[1–3]. The above mentioned mononucleotide deletion often occurs in the Bax microsatellite, a

[1]Department of Biology, Illinois Institute of Technology, 3101 South Dearborn Street, Chicago, IL 60616, USA. [2]Translational Research in Pediatric Oncology, Hematopoietic Transplantation and Cell Therapy, IdiPAZ Research Center, University Hospital of La Paz, Madrid, Spain. [3]IdiPAZ-CNIO Pediatric Oncohematology Clinical Research Unit, National Cancer Research Center (CNIO), Madrid, Spain. [4]Mass Spectrometer Core, University of Illinois at Chicago, Chicago, IL 60612, USA. ✉email: xiang@iit.edu

stretch of eight guanine (G8) repeats that is often subjected to mutations. The G8-to-G7 mutation is commonly detected in cancer patients with microsatellite instability (MSI)[6]. Furthermore, such stretch of nucleotide repeats is highly susceptible to alterations during the transcription and translation, such as transcriptional slippage and translational ribosomal frameshift[27].

Transcriptional slippage occurs when the RNA polymerase stops or stalls during DNA transcription, often in regions with repeat sequences[27]. The polymerase often "slips" and skips part of the sequence, either forward or backward[27]. Ribosomal frameshift (RFS) happens during translation; the ribosome stalls and skips one nucleotide either forward (+1RFS) or backward (-1RFS), subsequently translating the protein in a different reading frame[27–29]. The ribosomal frameshift mechanism is commonly used by viruses to generate different proteins using limited sequences[30]. However, only a few human genes have been described to use a similar mechanism to regulate protein levels in response to specific cellular signals[30–32]. Antizymes are the representative example, as intracellular polyamine levels function as a molecular switch to turn on or off a +1RFS for read-through antizyme translation[32–35]. It is also known that +1RFS can contribute to the aberrant forms of beta-amyloid precursor protein APP^{+1} in AD and other neurodegenerative diseases[27,36,37]. In this study, we identified RFS as an alternative mechanism for producing BaxΔ2 protein, replacing the Bax G8-to-G7 microsatellite mutation. This RFS-generated alternative isoform is named as BaxΔ2(G8)-RFS (Genebank Accession# PP524759) to distinguish the original BaxΔ2 isoform, which we updated the GeneBank annotation and renamed as BaxΔ2(G7) (Genebank Accession# JX524562.1).

Results

The G7 microsatellite mononucleotide deletion is not essential for BaxΔ2 expression

We recently detected a significant increase in BaxΔ2 protein levels in the brains of Alzheimer's disease (AD) patients[14]. The BaxΔ2(G7) has a G8-to-G7 mononucleotide deletion, predominantly detected in MSI cancer patients[5]. However, it was not clear whether such a "G8-to-G7" mutation is common in AD patients. To explore whether the mechanism driving BaxΔ2 production in AD parallels that observed in cancer, we performed a comprehensive analysis at both RNA and protein levels using samples (RNA, fresh-frozen tissue, and formalin-fixed paraffin-embedded tissue slides) obtained from the brain of an 85-year-old female AD patient. At the protein level, immunostaining of the frontal lobe tissues detected strong BaxΔ2-positive cells in the neurons of the AD patient, but not in the control neurons (Fig. 1a), consistent with what we observed previously[14]. BaxΔ2 protein was also distinctly detected in the AD brain fresh-frozen tissue through immunoprecipitation using anti-Bax antibody (P19, the epitope shared by both Baxa and BaxΔ2) followed by immunoblotting with anti-BaxΔ2 antibody (2D4, the epitope is specific for BaxΔ2 but not Baxα[10,11,14]) (Fig. 1b). To examine Bax exon 2 splicing, the RT-PCR result showed a smaller gel band compared to the Baxα control, but of a similar size to the BaxΔ2 control, suggesting the possibility of the exon 2 deletion. The sequencing analysis confirmed the exon 2 splicing and the microsatellite poly G mutations in this patient (Fig. 1c, Supplementary Fig. 1c and d). We previously detected that a striking high rate (85%) of AD patients exhibit Bax exon 2 alternative splicing using the ROSMAP AD brain RNA-seq dataset (ID: syn8612097)[14]. Upon further investigation of the Bax microsatellite status in the same AD RNAseq pool, it was revealed that only 5% of Bax transcripts with the exon 2 alternative splicing harbored the microsatellite G7 mutation (Fig. 1d, Supplementary Fig. 1d). These results indicate that the low rate of G7 mutation is inconsistent with the BaxΔ2 protein levels detected in the clinical samples[14], since BaxΔ2(G8) results in premature termination unless rescued by G8-to-G7 deletion to generate viable isoform, BaxΔ2(G7) (Fig. 1e). Therefore, other alternative mechanisms that allow the production of BaxΔ2 protein in the context of AD should be considered. Here we propose one possible mechanism via ribosomal frameshift (RFS), which can substitute the "G8-to-G7" mutation in production of an alternative BaxΔ2 isoform, BaxΔ2(RFS) (Fig. 1e).

Ribosomal frameshift is an alternative mechanism to produce BaxΔ2 protein

To investigate if a +1RFS compensates the G8-to-G7 microsatellite mutation in the production of BaxΔ2 in the context of AD, we performed the well-established ribosomal frameshift dual-luciferase assay[38]. Two luciferases at 5' and 3' ends were in-frame fused with a pre-spliced BaxΔ2 variant (exon 1 to exon 3) with either G7 or G8 microsatellite (Fig. 2a). The BaxΔ2 (G8, E1-3) construct would be out-of-frame, resulting in premature termination unless a +1RFS occurs, allowing for translation through the luciferase at the 3' end (*F luc*, Fig. 1a). As a control we used BaxΔ2(G7,E1-3), an in-frame construct that can translate through without the need for a frameshift. The vector alone was used as a negative control. Out-of-frame Bax exon 4, which has a similar length to the pre-spliced E1-3 contruct, was used as a mock control. All constructs were subjected to cell-free in vitro transcription/translation (IVTT) assay. The results showed that translational read-through rate of BaxΔ2(G8,E1-3) was significantly higher than the vector and E4 mock control (Fig. 2b). To verify this in a cellular system, we used a dual-tagged construct that allowed detection of the N- and C-terminus through immunofluorescence staining (Fig. 2c). The N-terminal Flag-tag and C-terminal HA-tag were fused with a BaxΔ2 construct consisting of exons 3–5 with G8 microsatellite(G8,E3-5). BaxΔ2(G7,E3-5) construct served as the in-frame control. Of note, the N-terminus (encoded by exon 1) was removed due to its instability, often resulting in the loss of the Flag-tag required for detection (Supplementary Fig. 2a and b). The C-terminus (encoded by exon 6) was also removed to reduce cytoxicity[7]. Expression of these constructs was tested in transfected neuronal HT22 cells. In the G7 control, double-positive cells were readily detected, as no frameshift was needed. For the G8 construct, the presence of double-positive cells indicated that +1RFS indeed occurred, allowing for read-through. However, we were unable to do a reliable quantitative analysis due to the weak signals and low number of double-positive cells. To further confirm the expression of the complete protein, we expressed BaxΔ2(G7 or G8,E3-5,) constructs in HT22 neuronal cells and immunoblotted with N-terminal BaxΔ2 specific 2D4 and C-terminal HA antibodies (Fig. 2e). The results showed that the BaxΔ2(G8,E3-5) was detected by both N-terminal and C-terminal antibodies (Fig. 2f) with 27% of read-through rate (Fig. 2g). Combination of the

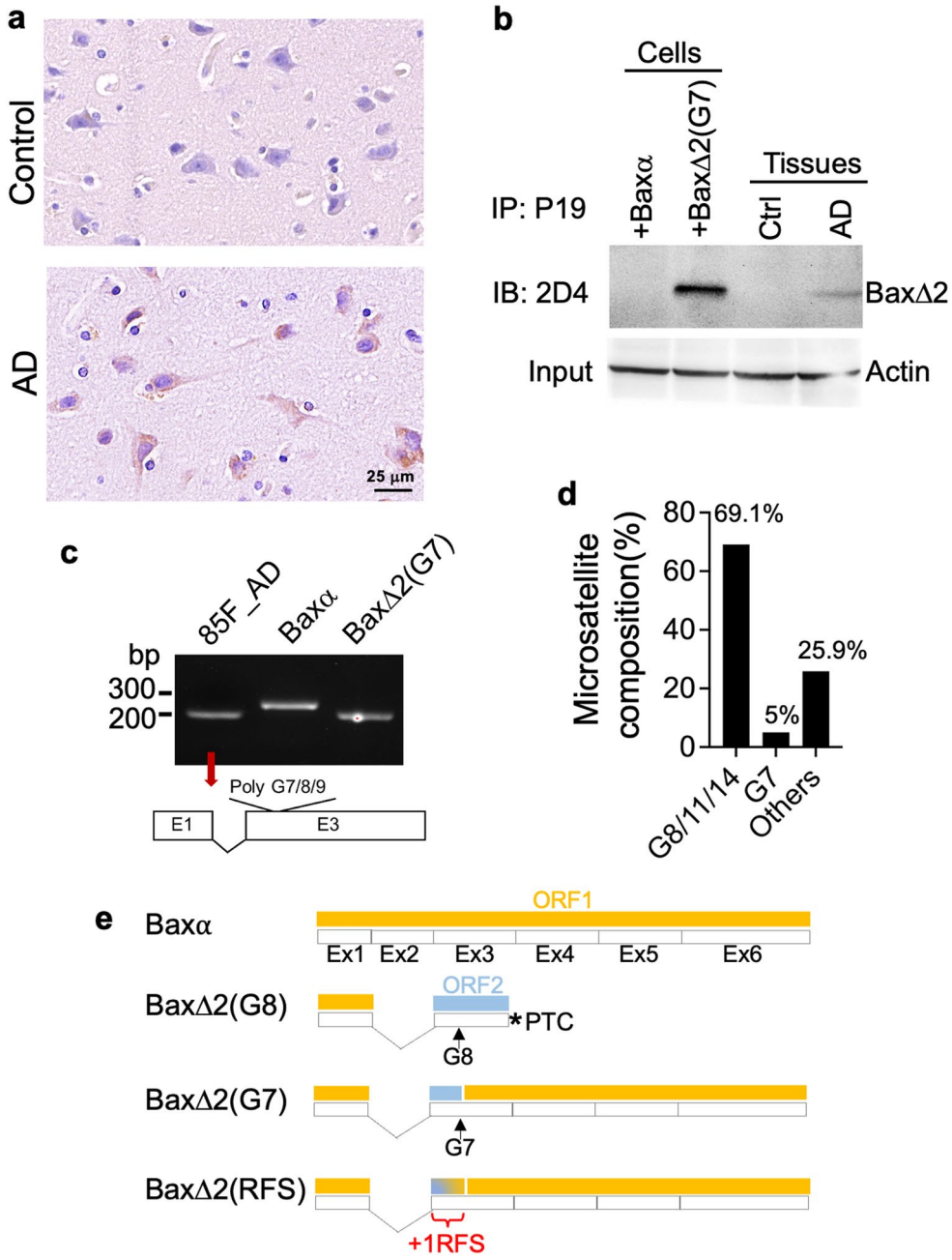

Figure 1. Bax G7 microsatellite mononucleotide deletion is not essential for BaxΔ2 expression. (**a**) Human brain frontal lobe tissue was immunohistochemically stained with 2D4 (anti-BaxΔ2 antibody). Images were from two individuals (a 54-year-old male control subject and an 85-year-old female AD subject). Scale bar, 25 μm. (**b**) HT22 neuronal cells transfected with Baxα or BaxΔ2 as controls and tissues from the same subjects in (**a**) were subjected to immunoprecipitation (IP) with anti-Bax antibody P19. The immunocomplexes were analyzed by immunoblotting (IB) with 2D4. Actin levels were used as an input control. The blot was cut prior to the hybridization. Original blots are shown in Supplementary Fig. 1a. (**c**) Total RNAs ofAD tissue and cells from (**b**) were subjected to RT-PCR. The Bax transcripts covering exon 1-3 were detected by gel electrophoresis. The arrow indicates the exon 2 splicing and the percentages of microsatellite poly G composition. Original gel is shown in Supplementary Fig. 1b. The sequence and the microsatellite poly G status are shown in Supplementary Fig. 1c and d, respectively. (**d**) Quantitation of the poly G microsatellite mutations within the AD RNA-seq dataset examined (n = 327). G8/11/14: G8, G11, and G14 have the same reading frame. (**e**) Schematic representation of reading frames for Baxα, BaxΔ2(G8), BaxΔ2(G7), and proposed BaxΔ2(RFS) (ribosomal frameshift) isoform. PTC, premature termination codon; Ex, exon; ORF, open reading frame.

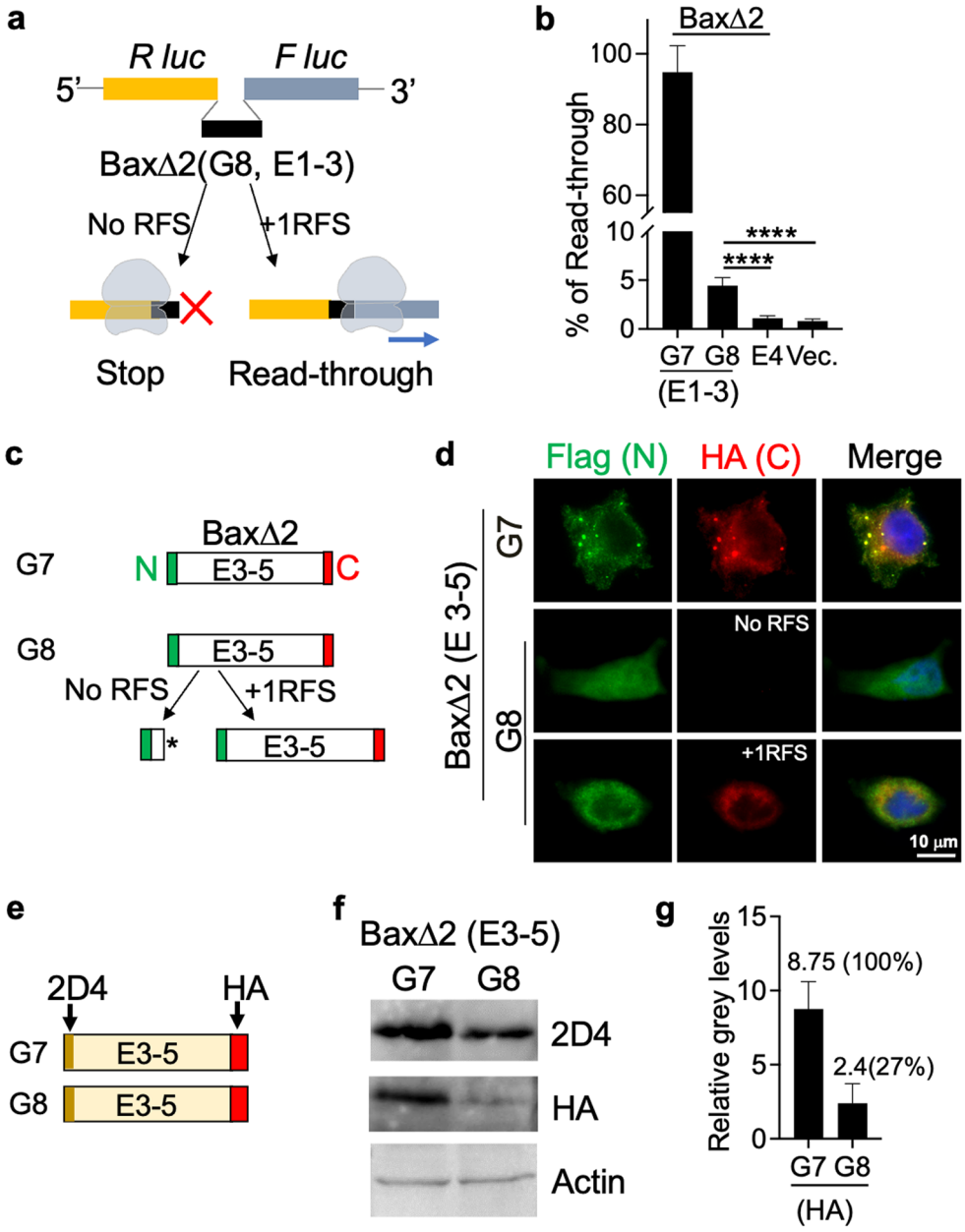

Figure 2. Ribosomal frameshift serves as an alternative mechanism for BaxΔ2 protein production. (**a**) Diagram indicating the possible outcomes of dual-luciferase assay with or without frameshift. E1-3, BaxΔ2 exon 1 and 3 with G8 microsatellite; *R luc*, Renilla luciferase; *F luc*, firefly luciferase. (**b**) Dual-luciferase activities from *in vitro* transcribed/translated products from (a); controls: E4, BaxΔ2 exon 4 (out of frame); Vec., empty dual-luciferase vector (out of frame). Statistical significance was calculated with one way ANOVA followed by Tukey's multiple comparisons test. Error bars represent standard deviation (SD). ****, $p < 0.0001$. (**c**) Diagram of reading frameshift assay with two-tagged constructs (N-terminal Flag tag, green, and C-terminal HA tag, red). E3-5, BaxΔ2 exon 3 to 5. (**d**) Immunofluorescence staining of HT22 cells transfected with the two-tagged constructs indicated in (b). Scale bar, 10 mm. (**e**)Diagram of constructs and antibodies used to detect reading frameshift through immunoblot. Antibody recognition sites were labeled on the top. (**f**) Immunoblotting of HT22 cells transfected with antibodies indicated; Original blots are shown in Supplementary Fig. 3; (**g**) quantitation of the intensity (grey scale) of bands from three independent HA immunoblots. The percentage of read-through was calculated with G7 control as 100%. Error bars represent SD. The quantitation of the bands for 2D4 antibody is shown in Supplementary Fig. 3e.

results from three different assays confirmed that + 1RFS can occur and compensate the lack of G7 mutation in the production of BaxΔ2 protein.

BaxΔ2 ribosomal frameshift appears to rely on RNA structure rather than primary microsatellite sequence

In the original BaxΔ2(G7) isoform, the microsatellite G8-to-G7 mutation is required and it is the site where the shifted reading frame caused by exon 2 splicing is restored[5,6]. We hypothesized that the same site at the microsatellite could serve as the + 1RFS site, as the stretch of guanine repeats is susceptible to ribosomal stalling and slippage, and the RNA/protein structure and microsatellite-downstream sequence could also influence this process[27]. To test this hypothesis, we generated three mutants of the BaxΔ2(G8,E3-5) construct: mutant (mt1), introducing a small alteration to the microsatellite consecutive poly G; mt2 replacing the potential frameshift region within and beyond the microsatellite; and mt3 disrupting only the microsatellite (Fig. 3a). The immunoblot results showed that full translation still occurred in mt1, suggesting the repetitive stretch of poly Gs is not essential for + 1RFS (Fig. 3b). However, both mt2 and mt3 failed to translate through, suggesting + 1RFS was impaired. Of note, the mt1 (from ggg ggg gga to gga gga gga) disrupts the polyG repeat but does not alter the amino acid sequence (both WT and mt1 code for Gly Gly Gly). On the other hand, mt3 not only disrupts the polyG repeat but also changes the amino acid coding (from Gly Gly Gly to Ala, Ala, Ala). The combined results from mt1 and mt3 suggest that the primary polyG sequence may not be critical. Instead, the frameshift process may be influenced by mutation-induced changes in RNA sequence, and/or by the change in the amino acid sequence caused by the mutation. Given that ribosomal frameshift often relies on RNA structure[27], we also predicted the RNA structures for all these mutants. We found that the local RNA structures of the failed mutants were dramatically different. Mt1 was able to maintain a similar stem structure as the control (ctrl), whereas mt2 and mt3 showed altered the stem structure with additional hairpin loops (Fig. 3c). These results suggest that the poly-guanine stretch repeat of the microsatellite is not essential for the BaxΔ2 ribosomal frameshift. Instead, it appears that the local RNA structure and/or amino acid sequence could be critical for + 1RFS to produce BaxΔ2 protein in the absence of the G7 mutation.

BaxΔ2 ribosomal frameshift occurs at a site 15 base pairs upstream of the microsatellite

As both the BaxΔ2 specific antibody (2D4) and the general Bax antibody (D2E11, against Leucine shared by both Baxa and BaxΔ2) can recognize the frameshifted BaxΔ2[14,39], this indicated that the + 1RFS site is located within the sequence region coding for the 16 amino acids between these two antibody's recognition epitopes (Fig. 4a). We predicted all possible outcomes from the + 1RFS in this region (Fig. 4a). To pinpoint the exact frameshift site, we performed immunoprecipitation-mass spectrometry (IP-MS) to enrich targeted proteins. HT22 neuronal cells were transfected with BaxΔ2(G8,E3-5) tagged with HA at the C-terminus and immunoprecipitated with anti-HA antibody covalently conjugated to agarose beads (Fig. 4b). The immunocomplex proteins were eluted from the beads and validated by both co-immunoprecipitation-immunoblot (Fig. 4c) and Coomassie staining (Fig. 4d). The results showed that the frameshifted BaxΔ2 proteins were pulled down and purified with minimal contamination. The eluted sample was subjected to MS analysis and the results showed a clear separation and signal intensity, with the best hit showing 87% sequence coverage under 1% False Discovery Rate threshold for peptide and protein filtering (Supplementary Fig. 4c). The + 1RFS site was identified at the adenine 15 base pairs upstream of the G8 microsatellite (Fig. 4a indicated by an asterisk). This new BaxΔ2 is named BaxΔ2(G8)-RFS (GenBank accession number PP524759). As a result, the peptide SSRAN in the original BaxΔ2(G7) isoform is changed to RAGRM in BaxΔ2(G8)-RFS (Fig. 4e). The rest of the protein sequence remains the same, including the critical epitope for the 2D4 antibody. These results provide conclusive evidence that BaxΔ2(G8), initially anticipated as a premature truncated form, can produce a functional BaxΔ2 protein using the + 1RFS mechanism in neuronal cells.

Discussion

Ribosomal frameshift occurs during translation when the ribosome "skips" one nucleotide either forward (+ 1) or backward (-1). This mechanism is very commonly used in viruses and bacteria for generating multiple proteins from a single gene[27–30]. Ribosomal frameshift events generally require a signal to stop or stall the ribosome during translation[27]. Bax exon 2 alternative splicing could cause a change in the RNA structure, which may fulfill the signal requirement for the + 1RFS. It is well-known that the mechanism underlying − 1RFS is generally signaled by RNA superstructure[27], while + 1RFS is less known. Evidence showed that RNA structure and RNA/amino acid interactions at the ribosome exit tunnel can control + 1RFS[27]. This led us to wonder if the reading frameshift might depend on, at least in part, local RNA structure. Our results in manipulating the microsatellite region (Fig. 3) supported this notion. Structural changes that affect RNA structure can be caused by multiple factors, which may be generated during AD development. Further work is needed to identify the factors including both *cis* and *trans* factors, which can influence the RNA structure that promote this + 1RFS.

One limitation of our study is that the results presented here may not fully reflect the in vivo intracellular conditions and environment. Due to the limitations of the size-efficiency of the dual tag assay systems and BaxΔ2 instability and cytotoxicity, we had to use truncated constructs. The C-terminus coded by exon 6 was removed due to its cellular toxicity. We have previously shown the a9 helix is responsible for activating both caspase-8 and stress granule-mediated cell death[8,9]. The N-terminal region encoded by exon 1 was also removed from most experiments since it is highly unstable and can get easily cleaved and degraded during the experiments, leading to loss of detection of the N-terminal tag (Supplementary Fig. 2). Although the remaining core region coded by exon 3–5 was sufficient for us to demonstrate the frameshift site, we noticed that its ability to form protein aggregates was weaker than the original BaxΔ2(G7) (Fig. 2d) for an unknown reason. We also noticed smaller bands below the predicted-size band on the BaxΔ2(G8,E3-5) blots (Supplementary Fig. 3). Although

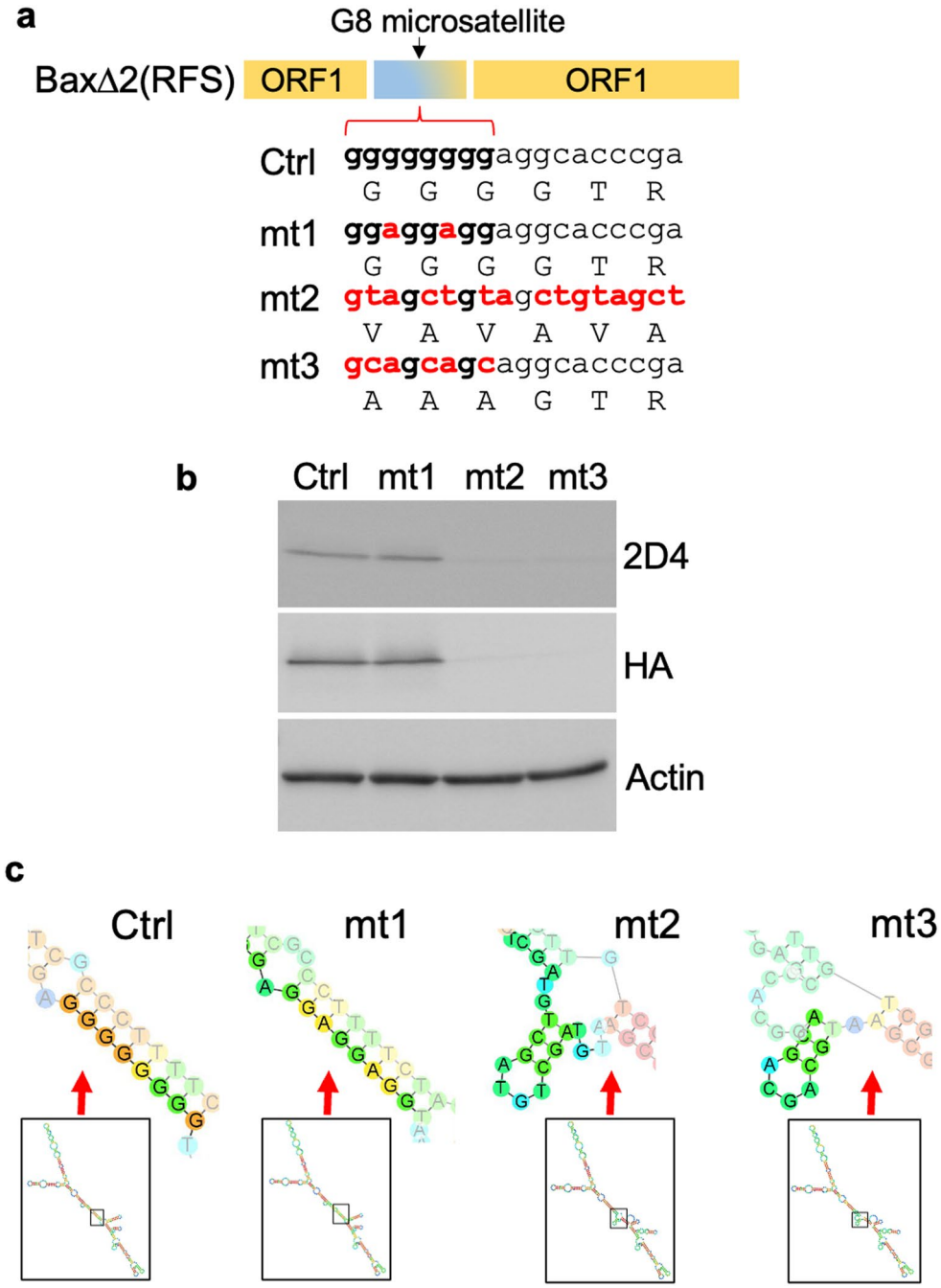

Figure 3. BaxΔ2 microsatellite poly G sequence is not essential for ribosomal frameshift, but its RNA structure potentially dictates the frameshift. (**a**) Comparison of the BaxΔ2 microsatellite regions among control (ctrl), mt1, mt2, and mt3. Microsatellite sites were bold, mutated nucleotides were colored as red. Translated amino acid sequences are listed below nucleotide sequences. (**b**) Immunoblotting of HT22 cells transfected with the constructs indicated in (a) using antibodies indicated (all constructs used here are based on BaxΔ2 E3-5 in Fig. 2e). The original blots and replicated blots are shown in Supplementary Fig. 4. (**c**) RNA structure prediction of BaxΔ2 microsatellite regions (arrow indicated enlarged region) in (a) and (b).

the reasons are unclear, this is likely due to the instability and degradation of the truncated proteins detected by the C-terminal HA antibody. It is unlikely to be caused by internal initiation, as we did not observe similar phenomena in the case of the BaxΔ2(G8, E1-5) construct (Supplementary Fig. 2).

Microsatellite mutations are well-documented in cancer patients with microsatellite instability (MSI-H), which have defects in the mismatch repair system, about 90% of hereditary nonpolyposis colorectal cancers (HNPCC) have Bax microsatellite mutations[40]. Other than that, about 15% of cells in tumors and 5% in normal tissues contain the Bax microsatellite G7 mutation[5,11]. However, the prevalence of microsatellite instability and the mutation rate of Bax are less explored in neurodegenerative diseases, such as Alzheimer's disease. Our

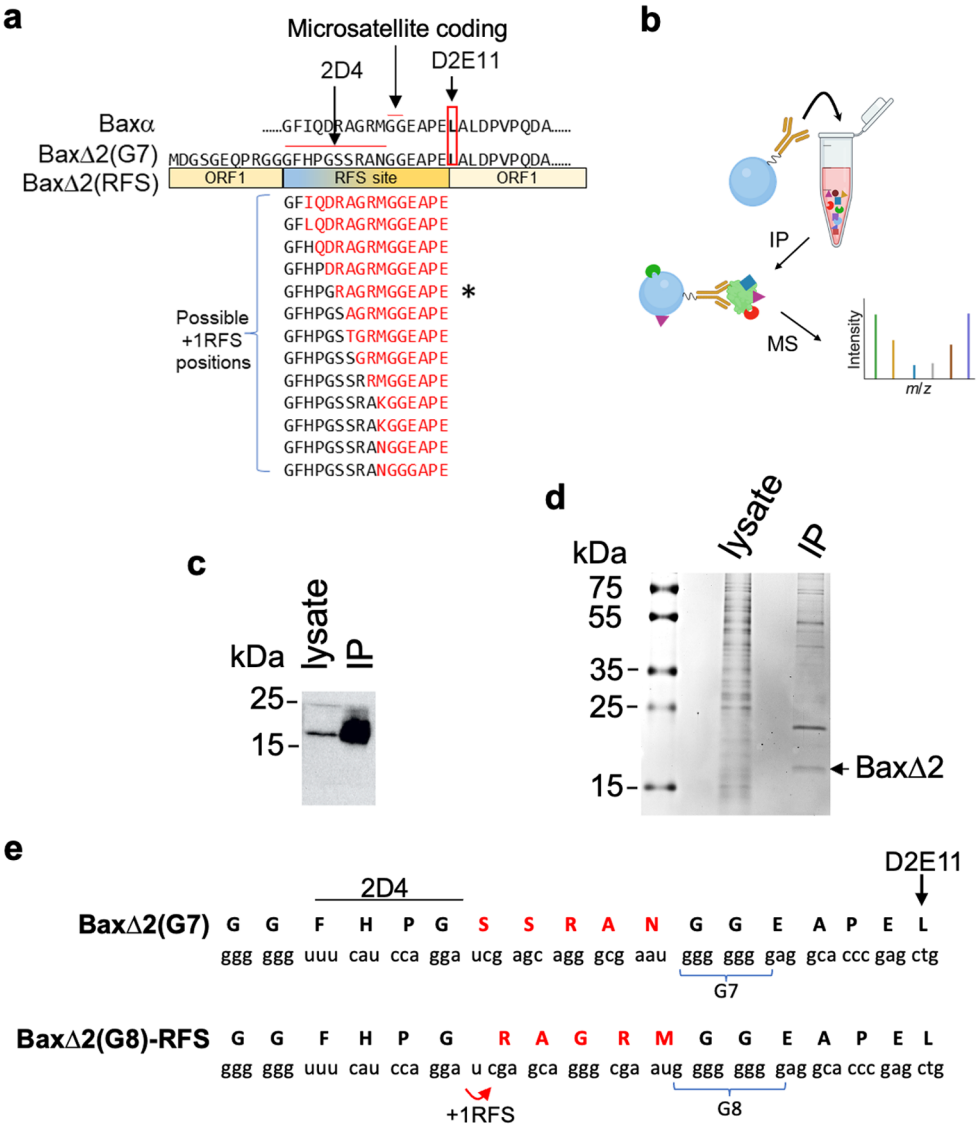

Figure 4. BaxΔ2 ribosomal frameshift occurs at the upstream nearby the microsatellite. (**a**) Predictions of potential BaxΔ2 post-frameshifted amino acid reading frames (new reading frames were labeled as red). The antibody recognition sites for 2D4 and D2E11 were labelled. (**b**) Diagram of the immunoprecipitation (IP) procedure for mass spectrometry (MS) sample preparation. HT22 cells were transfected with BaxΔ2(G8,E3-5) with HA tagged at the C-terminus. The cell lysate was pulled down with agarose beads conjugated with HA antibody. (**c** and **d**) Validations of the IP pull-down samples by immunoblotting (c) and Coomassie blue staining (d) Original gel and blot are shown in Supplementary Fig. 4b. (**e**) Sequence comparison between BaxΔ2(G7) and BaxΔ2(G8)-RFS isoforms covering their distinguished amino acid sequences (in red); the frameshift site (+1RFS) is marked below the sequence and an asterisk in (a). The full mass spectrometry BaxΔ2 amino acid sequence is shown in Supplementary Fig.4c.

previous work showed that the G7 microsatellite mutation rate was about 5% in AD[14]. Intriguingly, the length of the Bax microsatellite repeat in the AD samples varied widely from G7 to G11 (Supplementary Fig. 1d and e). Most of these transcripts will result in outframe and premature termination unless a ribosomal reading frameshift occurs to restore the reading frame, for example G8, G11, and G14 need + 1RFS, and G9 and G12 need − 1RFS. Future work should address the possibility of a -1RFS for BaxΔ2 in neurons. In conclusion, our work shows that ribosomal frameshift provides flexible alternatives to ensure the production of Bax variants regulated at the translational level. Such flexible alternatives provide an even greater "plasticity" for the Bax family members to excel in their pro-death function under various cellular contexts and conditions.

Methods

Materials and reagents

Postmortem human brain formalin-fixed paraffin-embedded tissue sections were obtained from BioChain. There was no live human subject involved in this study and the using of these human tissues in this study was

exempted by the Institutional Review Board (IRB) at the Illinois Institute of Technology (Legacy-IRB-2019-017). Antibodies against Bax (D2E11), HA, and Flag were purchased from Cell Signaling Technology; Bax (P19, recognizing both Baxa and BaxΔ2) was purchased from Santa Cruz Biotechnology; anti-HA agarose was purchased from Thermo Fisher Scientific. The BaxΔ2 monoclonal antibody (2D4) was generated previously against the sequence GFHGSSRANG, which is unique to BaxΔ2, and was well characterized with no cross-reactivity with Baxα in either immunostaining or immunoblotting[10,11,14,39]. The murine hippocampal neuronal cell line HT22 was obtained from Kerafast, Inc, Shirley, MA. The pSGDluc vector was a generous gift from Dr. JF Atkins (The University of UTAH). All methods used in this study were carried out in accordance with relevant guidelines and regulations.

Cloning of BaxΔ2 truncated and mutant constructs

The BaxΔ2 truncated constructs were generated through PCR-based cloning using BaxΔ2 as a template. BaxΔ2 truncated constructs: the first 190 bp of BaxΔ2 cDNA, comprising exons 1 and 3 (E1-3) with either the G7 or G8 microsatellite or BaxΔ2 exon 4 (171 bp's) were cloned into the dual-luciferase pSGDluc vector for luciferase assay. BaxΔ2(G7,E3-5) and BaxΔ2(G8,E3-5) with C-terminal Flag-tag or/and N-terminal HA-tag were cloned into pcDNA3.1 vector for immunoblotting and immunostaining. Microsatellite mutant constructs as indicated in the text were generated by fusion PCR. All constructs were verified by DNA Sequencing. All constructs used in this study were listed in Supplementary Fig. 5.

Cell culture and transfection

HT22 murine hippocampal neuronal cells were cultured in Dulbecco's Modified Eagle Medium (DMEM) supplemented with 10% fetal bovine serum (FBS). For transfection, cells were seeded in 6-well plates and grown to approximately 60% confluence before being transfected with BaxΔ2 truncated constructs using Lipofectamine 3000 reagent, sourced from Invitrogen (Waltham, U.S.). Cells were then incubated for the appropriate time corresponding to each experiment needs indicated in the text before downstream analysis.

Immunostaining and immunoblotting

Immunohistochemical staining of tissue slides with anti-2D4 antibody was performed the same as for previous publications[11,14]. Stained slides were scanned using a CRi Pannoramic Scan Whole Slide Scanner at the Integrated Light Microscopy Core Facility at the University of Chicago, and visualized using Pannoramic Viewer 1.15.2. For immunofluorescent staining, transfected cells on glass cover slides were stained with primary antibodies 2D4 (1:100), HA (1:100), or Flag (1:100) as described previously[11,14]. Fluorescent images were obtained using a Keyence BZ-X710 All-in-One Fluorescence Microscope and analyzed by ImageJ v1.52d. Immunoblotting was performed as described previously[11,14] with the following antibody specification for antibody dilutions (D2E11 1:1000; 2D4 1:200; HA 1:1000; Flag 1:1000; or actin 1:3000).

In vitro transcription and translation and dual-luciferase assay

In vitro transcription-translation (IVTT) assay was performed using TnT Quick Coupled Transcription/Translation System by Promega. The reaction was incubated for 90 min at 30 °C. The IVTT products were immediately used for the luciferase assays using the Dual-Glo luciferase assay kit (Promega) and activities were measured by GloMax 20/20 Luminometer (Promega) according to the manufacturer's instruction[38].

RNA isolation and sequencing

Total RNA was isolated from frozen tissue samples (Biochain) using the PureLink RNA Mini Kit (Life Technology) according to the manufacturer's instructions. The total RNAs were reversely transcribed to cDNAs using ThermoScript RT-PCR System (Invitrogen). The Bax transcripts were amplified from cDNAs with Bax primers to detect both Bax and BaxΔ2, 5'-ATG GAC GGG TCC GGG GAG CAG −3' (forward), and 5'-GTC CAC GGC AAT CAT CCT CTG C -3' (reverse). PCR products were separated through gel electrophoresis and sequenced at the University of Chicago Comprehensive Cancer Center (UCCCC) DNA Sequencing Facility.

RNAseq bax poly guanine analysis

AD brain RNA-seq dataset (ID: syn8612097)[41,42] together with clinical data and biospecimen metadata files from the ROSMAP study[43] (ROSMAP_clinical.csv, ROSMAP_CognitiveResilience_biospecimen_metadata.csv and ROSMAP_biospecimen_metadata.csv, respectively) were retrieved from the AD Knowledge Portal [database version:2023-02-20]. RNAseq dataset were mapped against Baxα and BaxΔ2 reference genes (GenBank accession numbers L22473.1 and JX524562.1, respectively) with minimap2 v2.21-r1071 through the get_SNPS.plv2.0f script from the SSRG pipeline (https://github.com/PombertLab/SSRG), details can be found in our previous publication[14]. The poly G sequences on BaxΔ2 isoforms were extrapolated from the presence of 7 or more guanines repeated in a row on each sequencing read per dataset as built in isoforms.pl v.0.7 (https://github.com/annecarolm/Publication_scripts/tree/main/2023_QYao_polyG).

RNA structure prediction

The RNA structure of BaxΔ2(G8) control and its mutants (mt1, mt2, and mt3) were predicted using RNA Andronescu 2007 from Geneious 10.0.5.

Immuno-precipitation and mass spectrometry analysis

Cell pellets were lysed in NP-40 buffer (145 mM NaCl, 5 mM $MgCl_2$, 1 mM EGTA, 0.25% NP-40, 20 mM HEPES, pH 7.4) with a cocktail of protease inhibitors at 4 °C for 30 min as described previously[12]. The cell lysate was incubated with 50 µl of anti-HA antibody conjugated agarose overnight at 4°C on a rocking platform.

Agarose immune-complexes were pelleted and washed twice with 500 µl of TBS-T (TBS with 0.05% Tween-20). The precipitated proteins were eluted with buffer containing 2% SDS, 5% glycerol, and 50mM Tris-HCl, pH6.8) and incubated 10 min at 50°C. After incubation, the supernatant was collected and added DTT at 50 mM. Eluted sample was verified by immunoblot and Coomassie staining before mass spectrum analysis. The eluted protein sample was analyzed using Q Exactive HF mass spectrometer coupled with an UltiMate 3000 RSLC nanosystem with a Nanospray Flex Ion Source (Thermo, Fisher Scientific) at the Mass Spectrometry Core at the University of Illinois Chicago.

Data availability

The datasets generated during the current study are available in the Github repository, (https://github.com/annecarolm/Publication_scripts/tree/main/2023_QYao_polyG).BaxΔ2(G8)-RSF mRNA sequence was deposited in GenBank accession number PP524759.

Received: 3 March 2024; Accepted: 10 October 2024
Published online: 08 November 2024

References

1. Yin, X. M., Oltvai, Z. N., Veis-Novack, D. J., Linette, G. P. & Korsmeyer, S. J. Bcl-2 gene family and the regulation of programmed cell death. *Cold Spring Harb. Symp. Quant. Biol.* **59**, 387–393 (1994).
2. Oltval, Z. N., Milliman, C. L. & Korsmeyer, S. J. Bcl-2 heterodimerizes in vivo with a conserved homolog, Bax, that accelerates programed cell death. *Cell* **74**, 609–619 (1993).
3. Chao, D. T. & Korsmeyer, S. J. BCL-2 FAMILY: regulators of cell death. *Annu. Rev. Immunol.* **16**, 395–419 (1998).
4. Chen, M. & Wang, J. Initiator caspases in apoptosis signaling pathways. *Apoptosis* **7**, 313–319 (2002).
5. Haferkamp, B. et al. BaxΔ2 family alternative splicing salvages bax microsatellite-frameshift mutations. *Genes Cancer*. **4**, 501–512 (2013).
6. Haferkamp, B. et al. BaxΔ2 is a novel bax isoform unique to microsatellite unstable tumors. *J. Biol. Chem.* **287**, 34722–34729 (2012).
7. Zhang, H. et al. Baxδ2 promotes apoptosis through caspase-8 activation in microsatellite-unstable colon cancer. *Mol. Cancer Res.* **12**, 1225–1232 (2014).
8. Xie, B., Yao, Q., Xiang, J. & Minh, D. D. L. A structural model for baxΔ2-mediated activation of caspase 8-dependent apoptosis. *Int. J. Mol. Sci.* **21**, 1–13 (2020).
9. Mañas, A. et al. The functional domains for BaxΔ2 aggregate-mediated caspase 8-dependent cell death. *Exp. Cell. Res.* **359**, 342–355 (2017).
10. Mañas, A., Davis, A., Lamerand, S. & Xiang, J. Detection of pro-apoptotic BaxΔ2 proteins in the human cerebellum. *Histochem. Cell. Biol.* **150**, 77–82 (2018).
11. Mañas, A. et al. Immunohistochemical detection of the pro-apoptotic BaxΔ2 protein in human tissues. *Histochem. Cell. Biol.* **154**, 41–53 (2020).
12. Basheer, S., Mañas, A., Yao, Q., Reiner, K. & Xiang, J. Detection of melanin-mediated false-positive for BaxΔ2 immunohistochemical staining in human skin tissues. *bioRxiv* **10**, 30.361956 (2020).
13. Mañas, A., Chen, W., Nelson, A., Yao, Q. & Xiang, J. BaxΔ2 sensitizes colorectal cancer cells to proteasome inhibitor-induced cell death. *Biochem. Biophys. Res. Commun.* **496**, 18–24 (2018).
14. Yao, Q. et al. Unconventional source of neurotoxic protein aggregation from organelle off-target BaxΔ2 in Alzheimer's disease. *Biomolecules* **13**(6), 970. https://doi.org/10.3390/biom13060970 (2023).
15. Vanderweyde, T., Youmans, K., Liu-Yesucevitz, L. & Wolozin, B. Role of stress granules and RNA-binding proteins in neurodegeneration: a mini-review. *Gerontology* **59**, 524–533 (2013).
16. Ash, P. E. A., Vanderweyde, T. E., Youmans, K. L., Apicco, D. J. & Wolozin, B. Pathological stress granules in Alzheimer's disease. *Brain Res.* **1584**, 52–58 (2014).
17. Ishunina, T. A. Chapter 12 - Alternative splicing in aging and Alzheimer's disease: Highlighting the role of tau and estrogen receptor α isoforms in the hypothalamus. *Handbook of Clinical Neurology* (eds. Swaab, D. F., Buijs, R. M., Kreier, F., Lucassen, P. J. & Salehi, A.) 182, 177–189 (Elsevier, Amsterdam, 2021).
18. Aranda-Abreu, G. E., Hernández Aguilar, M. E., Durán, F. R., Mestizo Gutiérrez, S. L. & Denes, J. M. Alternative splicing in alzheimer's disease. *Altern. Splicing Dis.* **2**, 39–50 (2016).
19. Biamonti, G. et al. Alternative splicing in Alzheimer's disease. *Aging Clin. Exp. Res.* **33**, 747–758 (2021).
20. Alam, S., Suzuki, H. & Tsukahara, T. Alternative splicing regulation of APP exon 7 by RBFox proteins. *Neurochem Int.* **78**, 7–17 (2014).
21. Liu, F. & Gong, C. X. Tau exon 10 alternative splicing and tauopathies. *Mol. Neurodegener*. **3**, 1–10 (2008).
22. Corsi, A., Bombieri, C., Valenti, M. T. & Romanelli, M. G. Tau isoforms: gaining insight into MAPT alternative splicing. *Int. J. Mol. Sci.* **23**, 15383. https://doi.org/10.3390/ijms232315383 (2022).
23. Apte, S. S., Olsen, B. R. & Mattei, M.-G. Mapping of the human BAX gene to chromosome and isolation of a novel alternatively spliced transcript, BAXS. *Genomics* **26**, 592–594 (1995).
24. Schmitt, E., Paquet, C., Beauchemin, M., Dever-Bertrand, J. & Bertrand, R. Characterization of Bax-σ, a cell death-inducing isoform of Bax. *Biochem. Biophys. Res. Commun.* **270**, 868–879 (2000).
25. Fu, N. Y., Sukumaran, S. K., Kerk, S. Y. & Yu, V. C. Baxβ: a constitutively active human bax isoform that is under tight regulatory control by the proteasomal degradation mechanism. *Mol. Cell.* **33**, 15–29 (2009).
26. Jin, K. L. et al. Bax κ, a novel Bax splice variant from ischemic rat brain lacking an ART domain, promotes neuronal cell death. *J. Neurochem*. **77**, 1508–1519 (2001).
27. Atkins, J. F., Loughran, G., Bhatt, P. R., Firth, A. E. & Baranov, P. V. Ribosomal frameshifting and transcriptional slippage: from genetic steganography and cryptography to adventitious use. *Nucleic Acids Res.* **44**, 7007–7078 (2016).
28. Advani, V. M. & Dinman, J. D. Reprogramming the genetic code: the emerging role of ribosomal frameshifting in regulating cellular gene expression. *BioEssays*. **38**, 21–26 (2016).
29. Ketteler, R. On programmed ribosomal frameshifting: the alternative proteomes. *Front. Genet.* **3**, 1–10 (2012).
30. Dinman, J. D. Programmed ribosomal frameshifting goes beyond viruses. *Microbe* **1**, 521–527 (2006).
31. Wills, N. M., Moore, B., Hammer, A., Gesteland, R. F. & Atkins, J. F. A functional –1 ribosomal frameshift signal in the human paraneoplastic Ma3 gene. *J. Biol. Chem.* **281**, 7082–7088 (2006).
32. Ivanov, I. P. & Atkins, J. F. Ribosomal frameshifting in decoding antizyme mRNAs from yeast and protists to humans: close to 300 cases reveal remarkable diversity despite underlying conservation. *Nucleic Acids Res.* **35**, 1842–1858 (2007).
33. Ivanov, I. P., Gesteland, R. F. & Atkins, J. F. A second mammalian antizyme: conservation of programmed ribosomal frameshifting. *Genomics* **52**, 119–129 (1998).

34. Howard, M. T. et al. Cell culture analysis of the regulatory frameshift event required for the expression of mammalian antizymes. *Genes Cells* **6**, 931–941 (2001).
35. Yordanova, M. M., Wu, C., Andreev, D. E., Sachs, M. S. & Atkins, J. F. A nascent peptide signal responsive to endogenous levels of polyamines acts to stimulate regulatory frameshifting on antizyme mRNA. *J. Biol. Chem.* **290**, 17863–17878 (2015).
36. Wills, N. M. & Atkins, J. F. The potential role of ribosomal frameshifting in generating aberrant proteins implicated in neurodegenerative diseases. *Rna* **12**, 1149–1153 (2006).
37. Saffert, P., Adamla, F., Schieweck, R., Atkins, J. F. & Ignatova, Z. An expanded CAG repeat in huntingtin causes +1 frameshifting. *J. Biol. Chem.* **291**, 18505–18513 (2016).
38. McNabb, D. S., Reed, R. & Marciniak, R. A. Dual luciferase assay system for rapid assessment of gene expression in Saccharomyces cerevisiae. *Eukaryot. Cell* **4**, 1539–1549 (2005).
39. Yao, Q. et al. Expression profile of the proapoptotic protein Bax in the human brain. *Histochem. Cell. Biol.* 209–220. https://doi.org/10.1007/s00418-022-02146-5 (2022).
40. De'angelis, G. L. et al. Microsatellite instability in colorectal cancer. *Acta Biomed.* **89**, 97–101 (2018).
41. Greenwood, A. K. et al. The AD knowledge portal: a repository for multi-omic data on Alzheimer's disease and aging. *Curr. Protoc. Hum. Genet.* **108**, 1–13 (2020).
42. Lee, A. J. et al. Multi-region brain transcriptomes uncover two subtypes of aging individuals with differences in the impact of APOEe4. *Alzheimers Dement.* **17**, e057240 (2021).
43. Bennett, D. A. et al. Religious orders study and rush memory and aging project. *J. Alzheimer's Dis.* **64**, S161–S189 (2018).

Acknowledgements

The AD RNAseq datasets were provided by the Rush Alzheimer's Disease Center, Rush University Medical Center, Chicago. ROSMAP is supported by the National Institutions of Health P30AG10161, P30AG72975, R01AG15819, R01AG17917. U01AG46152, and U01AG61356. The mass spectrometry analysis was performed by the Mass Spectrometry Core in Research Resources Center of University of Illinois at Chicago; the authors would also like to acknowledge the NIH s10 shared instrumentation grant (1S10OD027016-01) for supporting this work.

Author contributions

Conceptualization, J.X. and A.M.; Methodology, J.X., A.M., Q.Y., O.J., and H.C.; Experiment and data collection, Q.Y., A.M., E.B., A.C.M.D.S., and Y.Z.; Data analysis Q.Y., A.M., and J.X.; Writing original draft, Q.Y. and J.X.; Review and Editing, all authors. Resource: J.X. and H.C.

Declarations

Competing interests

The authors declare no competing interests.

Additional information

Supplementary Information The online version contains supplementary material available at https://doi.org/10.1038/s41598-024-76061-1.

Correspondence and requests for materials should be addressed to J.X.